

INTERNATIONAL SOCIETY FOR SOIL MECHANICS AND GEOTECHNICAL ENGINEERING



This paper was downloaded from the Online Library of the International Society for Soil Mechanics and Geotechnical Engineering (ISSMGE). The library is available here:

<https://www.issmge.org/publications/online-library>

This is an open-access database that archives thousands of papers published under the Auspices of the ISSMGE and maintained by the Innovation and Development Committee of ISSMGE.

The paper was published in the Proceedings of the 8th International Symposium on Deformation Characteristics of Geomaterials (IS-PORTO 2023) and was edited by António Viana da Fonseca and Cristiana Ferreira. The symposium was held from the 3rd to the 6th of September 2023 in Porto, Portugal.

Investigation of coated hydrophobic granular materials by means of computed tomography and environmental scanning electron microscopy

Clara Magalhães Toffoli^{1#}, Marius Milatz¹, and Jürgen Grabe¹

¹ Hamburg University of Technology (TUHH), Institute of Geotechnical Engineering and Construction Management, Germany

[#]Corresponding author: clara.toffoli@tuhh.de

ABSTRACT

Hydrophobic materials in geotechnical engineering and soil science can have natural or artificial origin. They can be applied, e. g., to waterproof structures in the industry. In this contribution, hydrophobic granular material was manufactured through a cold plasma polymer coating procedure. The monomer used was C4F8 (octafluorocyclobutane) and the material to be coated was Hamburg sand, a coarse grained sand. In this context, computed microtomography and environmental scanning electron microscopy were used to investigate the materials in their unsaturated state. The tools are applied to visualize unsaturated phenomena on the microscale. The hydrophobic and untreated materials were imaged by both techniques at different saturation degrees in order to understand the influence of the coating on the sample's hydraulic behaviour. The chosen environmental scanning electron microscope is able to provide relative humidity in the sample chamber, and so water drops were condensed on the grain surface, allowing to also observe the initial contact of water and the hydrophobic coating. It was observed how the capillary menisci, their geometry and contact properties evolve at different degrees of saturation. The measurements obtained and respective analyses state qualitatively the influence of the hydrophobic coatings on the pore water dynamics at different saturation degrees, which dictates the material's hydraulic behaviour. Contact angles were also analysed where it was physically possible.

Keywords: hydrophobic granular material; computed tomography; environmental scanning electron microscopy; contact angle.

1. Introduction

Geotechnical focused research on hydrophobic soil has been going on for several years. Instigated by its natural occurrence, geotechnical engineers and other scientists have studied those soils' origins, occurrence, properties, effects on other phenomena and also have modelled it (Jordán *et al.* 2013).

Traditionally, the variable that states if a material is hydrophobic or not is the contact angle θ . This angle is measured at the triple phase line, where air, water and soil get in contact at the same time. An equipment named goniometer is used to perform the Sessile Drop Method and measure the angle's value in the laboratory. Figure 1 depicts the contact angle measurement in an image obtained with the goniometer. If the angle is greater than 90° , the material is considered hydrophobic, otherwise, it is hydrophilic. As the technique was initially developed to be used for plain surfaces composed by only one material, it had to be adapted to be employed for sand, which is not plain and is composed of multiple grains made of different minerals (Liu and Lourenço 2019).

Another test that can be used for the classification of a sample in regarding its hydrophobicity is the water drop penetration time (WDPT). It consists in placing a drop with precise volume on the surface of the material and measuring the time it needs to penetrate completely.

Apart from natural occurrence, in which the hydrophobic soil is usually originated by forest fires or ground contamination, the material has also been intentionally manufactured. Intentional geotechnical use of hydrophobic soil is starting to be described in literature. Amongst its possible applications are slope covering, dam core, foundation impermeabilization etc. (Lourenço *et al.* 2018), even though currently the price of the technology still imposes limitations.

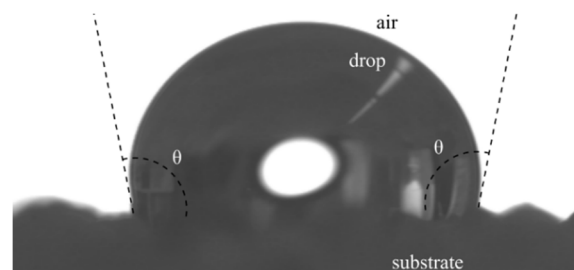


Figure 1. Contact angle measurement by the Sessile Drop Method (SDM).

In this context, given that sand grains are usually hydrophilic, because of the minerals they are composed of (Lourenço *et al.* 2015), different techniques have been used to hydrophobize the grains. The hydrophobic grain manufacture technique usually consists of mixing the air-dried material with a hydrophobic compound to coat the

grains. The chemical most commonly used in literature is dimethyl-trichlorosilane (DMS), in a technique named silanization. The use of polydimethylsiloxane (PDMS) and dichlorodimethylsilane (DMSCS) is also described.

As for unsaturated soil mechanics, the hydrophobic coating is expected to interfere with the apparent cohesion induced by the capillary bridges. Because of the contact angles that are theoretically larger than 90° , the capillary bridge is expected to have a convex shape instead of a concave, as observed for hydrophilic soils. The familiar concave shape is a consequence of the pressure gradient between pore air and bridge water, but also of the contact angle at the triple phase line, which is smaller than 90° . Theoretically, as a consequence, the convex capillary bridge connecting grains stops acting as a cohesive force and is supposed to start pushing the grains apart and lead to sample volume increase, instead of the decrease (Lourenço *et al.* 2018).

In this context, imaging technologies have been applied to better understand the interaction of water and grains coated with hydrophobic substances in different unsaturated states. Among them, micro computed tomography (μ CT) and environmental scanning electron microscopy (ESEM) were used. μ CT has already been employed to image unsaturated granular soil on the grain scale, as in Milatz *et al.* (2021). It was necessary to employ different equipment because each technology is more capable of evaluating a specific range of the materials unsaturated states.

2. Methodology

The soil used for the research described in this paper is sand coated with a hydrophobic polymer. This was achieved by means of a cold plasma technique, already familiar to the industry, in which the material to be coated and the monomer are inserted in a plasma chamber for a specific time interval (Zainal *et al.* 2015, Schoeter *et al.* 2021). The monomer used was octafluorocyclobutane (C4F8) and the soil is Hamburg Sand. Table 1 (Milatz *et al.* 2021) summarizes its properties: grain density (ρ_s), min. void ratio (e_{min}), max. void ratio (e_{max}), grain diameter at 10% passing (d_{10}), grain diameter at 50% passing (d_{50}) and max. grain diameter (d_{max}). The monomer has already been used in the industry, for example in the textile industry, to waterproof clothing (Cassie and Baxter 1944). In order to be able to compare the results, coated and non-coated material was employed.

Table 1. Hamburg sand properties

ρ_s [g/cm ³]	e_{min} [-]	e_{max} [-]	d_{10} [mm]	d_{50} [mm]	d_{max} [mm]
2.64	0.520	0.805	0.45	0.68	2.0

After the coated material was manufactured, the imaging phase of it in the unsaturated state started. Initially, to analyze how water drops form on the surface of coated initially hydrophobic material, an ESEM model Thermo Fisher Quattro was employed. This microscope is able to vary the relative humidity (RH) inside the sample chamber, a feature that was employed to condensate water on the material's surface. This feature stems from the equipment being able to operate on lower

vacuums than original ones. The RH is controlled via pressure and temperature. The microscope used detector was the gaseous secondary electron detector (GSED) and the beam voltage was 15 kV. Because ESEM images a 3D structure with a 2D image, it is not possible to directly measure the contact angle of the drop. Therefore, the criteria used in this contribution for stating that the material is behaving hydrophobically and thus that the contact angle is larger than 90° is that the drop has to be constituted by more than a whole hemisphere. Due to the same reasons, it is not possible to calculate the saturation degree of the sample analyzed by it.

The condensation procedure could also be achieved during CT imaging, but a special equipment would be required to induce drop condensation. If water was mixed with the sand or injected by means of a syringe, the drop condensation process would not happen, because the saturation degree variation would not be smooth enough.

For the funicular and pendular states of the unsaturated range, μ CT can be and was employed. The sample was prepared with a specific saturation degree by weighting the masses of sand and water, mixing them and then compacting the wet material in a sample holder with specific volume. As explained before, this process is only feasible for higher degrees of saturation.

The equipment used to obtain the images was a Scanco Medical μ CT 35. The energy used was 70 kVp (Kilovolt peak), 114 μ A, 8 W. Two sample holders were used: with 5 mm and with 10 mm in internal diameter. The height of the imaged volume was determined by how much of the sample's height was scanned. For both holders, 468 horizontal parallel 2D slices were obtained. The integration time was 600 ms and averaging was set to 2. This means that each reading was made twice and those were averaged. Lastly, the voxel size obtained for the smaller holder is 3.5 μ m, and for the bigger one, 10 μ m. For the segmentation of CT data, the software Avizo was employed. The process consists of segmenting the grayscale image in order to categorize each voxel in soil, water or air. Non-local means and median filters were used, and then 2D Histogram segmentation was employed. After that small spots were removed. At the end of the segmentation, saturation degree and void ratio can be calculated on the segmented images and confirmed. Avizo software is able to export a spreadsheet with the material properties per slice. This indicates if the void ratio and saturation degree intended while preparing the sample were achieved.

3. Results and Discussion

The images obtained by the ESEM clearly registered the samples wetting path via drop condensation. Figure 2 depicts the process for the coated sample and Figure 3, for the uncoated one. For the initial phase of the coated sample (Figure 2a-d), it is visible that the contact angle in the triple phase line is greater than 90° , as by the criteria exposed in section 2. In contrast, for the uncoated sample, which is hydrophilic, the contact angles of the forming drops are smaller than 90° since the beginning of the process. The magnification employed by the microscope during the process was 1949 or 300 times, as indicated in the images.

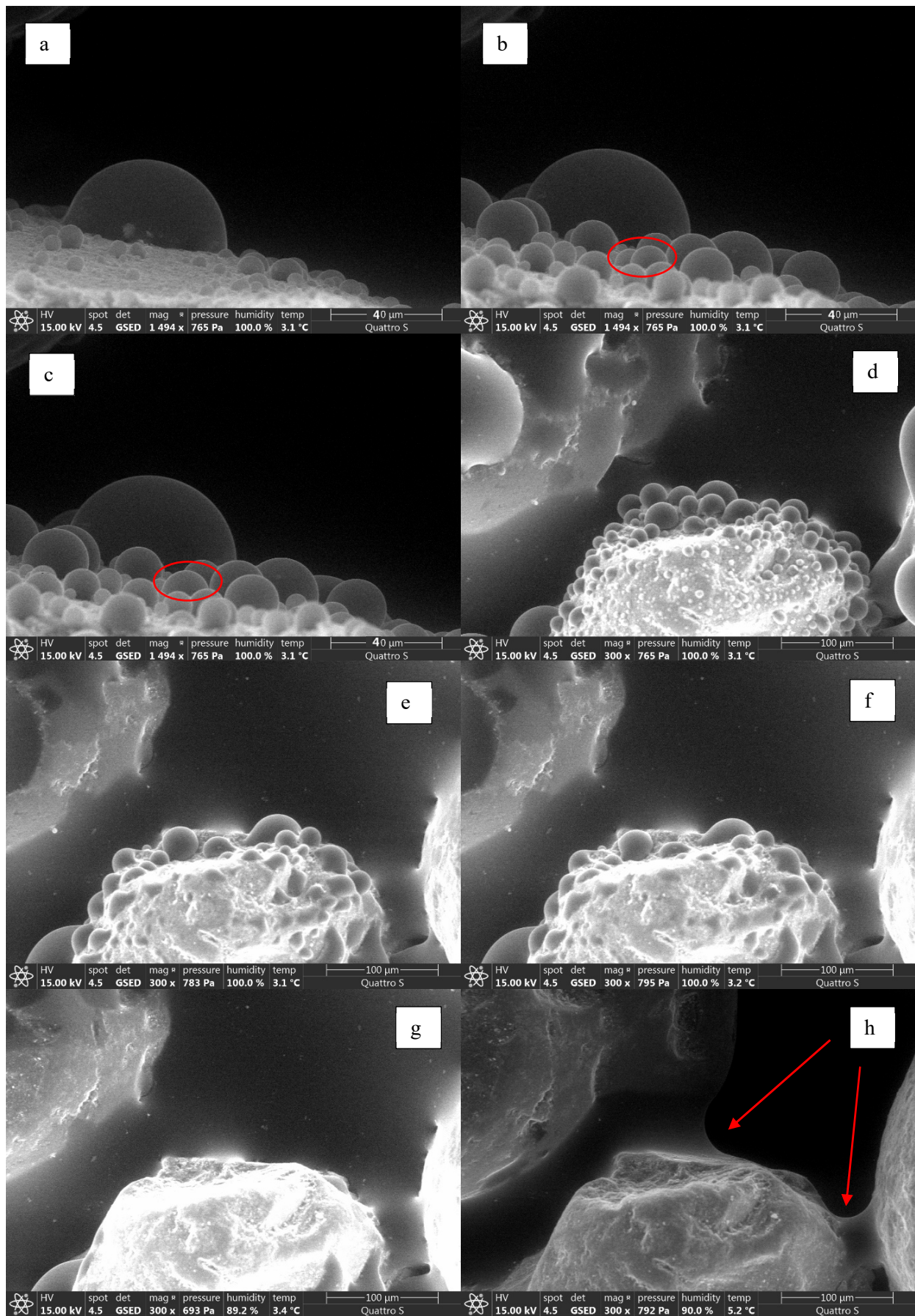


Figure 2. ESEM images of the coated grains during wetting process induced by water vapor. (a) is the beginning of the observed time while (h) is the end of it.

In the coated sample, as the drops get bigger, they start merging and forming even bigger ones. This is visible in Figure 2b-c, where the drawn circle specifically highlights the merge of two different drops. As this process takes place, it is noticeable that the contact angle is gradually reduced, coming to a point when drops are not formed by more than a full hemisphere anymore. At this point, it is noticeable that the contact angles are

smaller than 90° (Figure 2e-f), although they cannot be explicitly measured.

It was also observed that after the whole sand grain is covered by a water film (Figure 2g), menisci start to form and connect grains initially two-by-two (arrows in Figure 2h), entering the pendular state. It can be noticed that the contact angle of those menisci is also smaller than 90° . At this stage, the sample behaves in a hydrophilic manner.

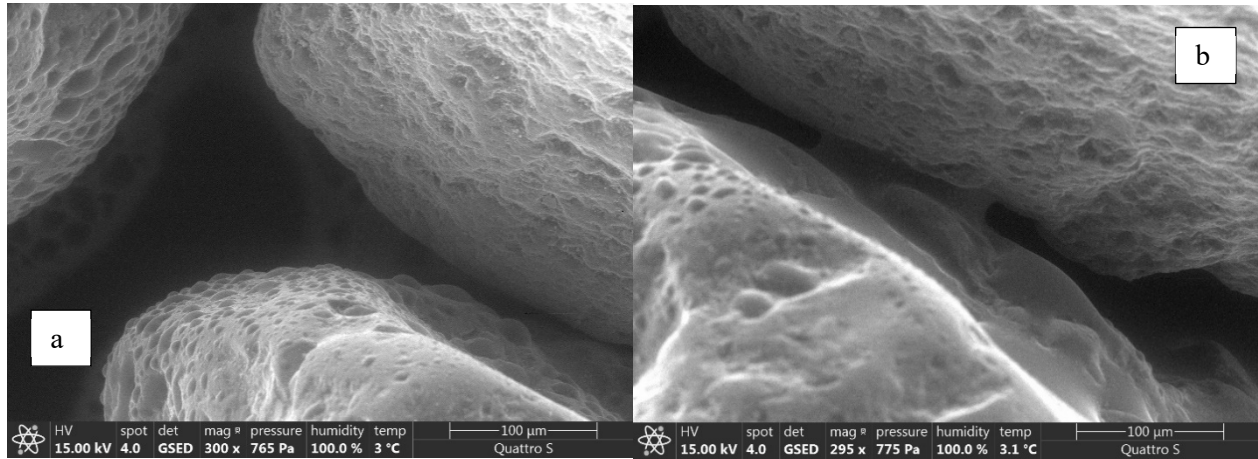


Figure 3. ESEM Images of the uncoated grains during wetting process induced by water vapor. (a) is the beginning of the observed time while (b) is the end of it.

For the uncoated sample, the drop formation process is similar, but the contact angle is smaller than 90° since the beginning of the condensation, as indicated in Figure 3a. During the meniscus formation connecting the two grains, visible in Figure 3b, the behaviour is similar to the one observed in the coated grain: both of them have contact angles smaller than 90° at this stage.

Figure 4 depicts one 2D slice of the CT scan of a C4F8 coated sand sample with 22% saturation degree and a void ratio of 0.561. The voxel size of the computed volume is $10\ \mu\text{m}$. Figure 5 presents the respective reconstructed 3D volume. Figure 6 depicts an image of a new sample of the same material with 50% saturation degree and a void ratio of 0.568. The smaller sample holder was employed in order to obtain higher resolution: $3.5\ \mu\text{m}$. Figure 7 depicts a similar CT image, but acquired from an uncoated sample with 40% saturation degree and a void ratio of 0.583. Its resolution is the same from Figure 6: $3.5\ \mu\text{m}$.

From Figure 4 to Figure 7 it is noticeable that the contact angles are smaller than 90° on their majority. With this imaging technology, it is possible to effectively measure the angle, given that the CT technique provides the view of the inner part of the sample without destroying it. Qualitatively analyzing, it is noticeable that the overall trend of the contact angles is the same in both images. A further statistical quantitative analysis is required in order to be able to evaluate differences between contact angle frequency distributions.

The WDPT index test results also point in the same direction. In the tests performed on the coated sample with a saturation degree greater than 5%, the drop immediately penetrated the substrate. This indicates that the material does not behave hydrophobically anymore, although it is coated with a hydrophobic substance.

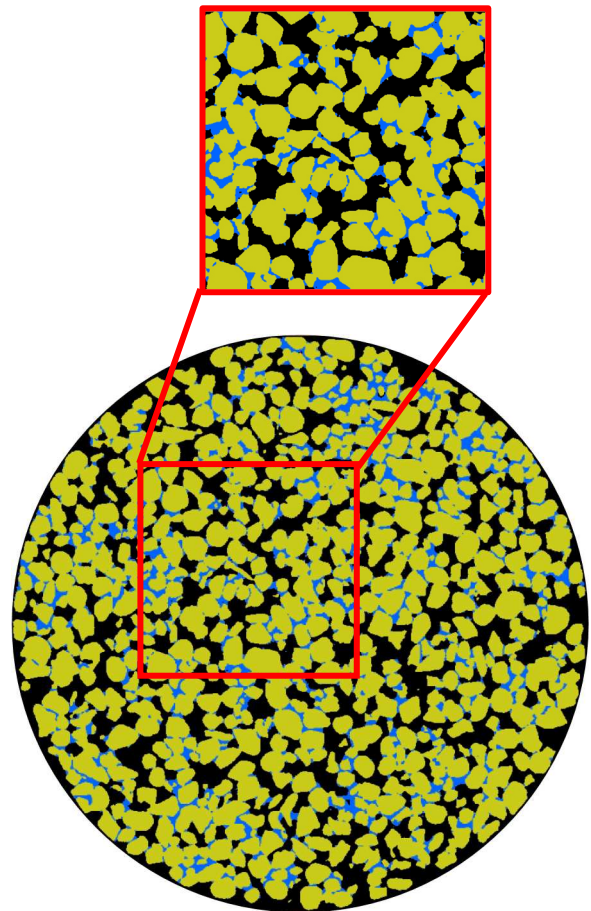


Figure 4. 2D μCT image of C4F8 coated sand at a saturation degree of 22%, voxel size of $10\ \mu\text{m}$.

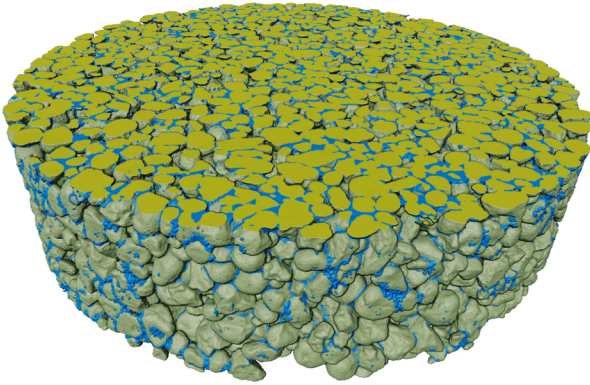


Figure 5. Reconstructed 3D volume of C4F8 coated sand presented in Figure 4.

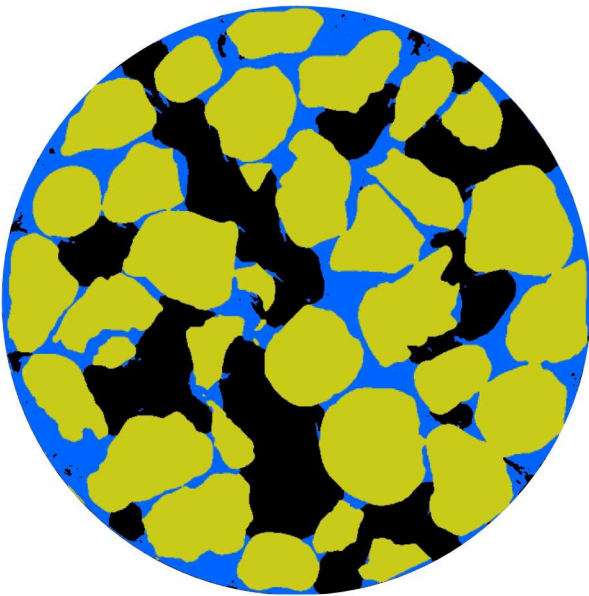


Figure 6. 2D μ CT image of C4F8 coated sand at a saturation degree of 50%, voxel size of 3.5 μ m.

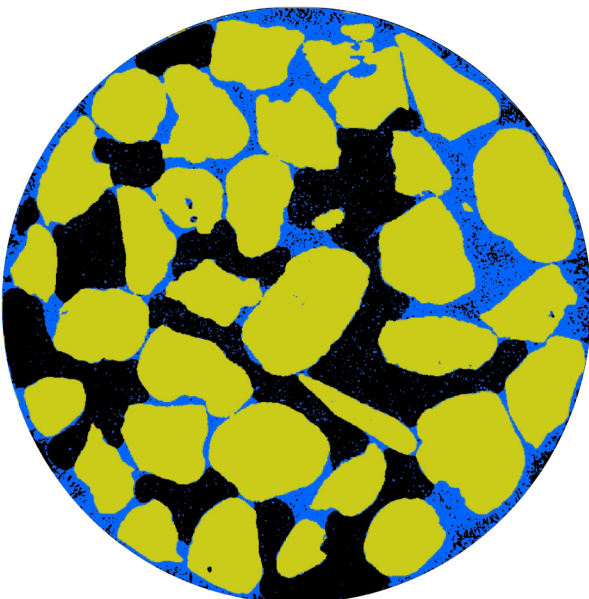


Figure 7. 2D μ CT image of uncoated sand at a saturation degree of 40%, voxel size of 3.5 μ m.

The main research question that this paper addresses is the changing pore scale wettability with saturation degree of coated initially hydrophobic material. As it is noticeable in the different unsaturated regime stages, achieved during ESEM and μ CT imaging, the wettability is strongly related to the already present water content, quantified in terms of the saturation degree, apart from other factors.

This change in behavior can explain why coated initially hydrophobic soils still develop apparent cohesion and experience a volume decrease as a response to suction, in a similar manner as uncoated hydrophilic material. As described in section 1, the expected behavior would be dilation, as an answer to the contact angle greater than 90° at the menisci triple phase line.

In summation, the coated sample behaves in a hydrophobic manner during the first contact of the dry hydrophobic surface with water. After that, added water starts interacting with the water already present, leading to concave menisci and a hydrophilic pore scale behavior. The variable that defines the behavior ranges, then, is the saturation degree or any other similar one that quantifies the water distributed in the pores.

4. Conclusion

This paper demonstrates by means of imaging technologies that sand grains coated with hydrophobic chemicals only behave in an expressive hydrophobic manner until a limited degree of saturation. For the case studied (Hamburg sand, C4F8 coating, the technique employed to coat the grains and its parameters) the boundary measured between the expressive hydrophobic behavior and its absence is a saturation degree of 5%. As it currently is, this could impose imitations to the intended applications.

This means that the expected triple phase line contact angle greater than 90° is only observed at the beginning of the wetting phase, performed in this study via drop condensation. When the pore space water starts to revolve the grains and form capillary bridges between them, the contact angle captured by ESEM and CT images is not greater than 90° anymore, characterizing hydrophilic behaviour. This is probably a consequence of this water interacting with the water film formed around the grain, and not with the hydrophobic coating anymore.

Statistical analysis of contact angles on images of both coated and uncoated material at different saturation degrees can provide the frequency distribution of the variable. This next step is already been executed by the authors and will allow the quantitative analysis of the hydrophobic coating influence.

In this study, CT was used alongside ESEM to allow a non-destructive 3D analysis of the samples. Although the ESEM chamber allows the drop condensation process, the measuring of contact angles, void ratio and saturation degree are not possible with this technology. In this context, a suggestion for the future of this research is developing a device to control the relative humidity inside the CT equipment, allowing to obtain CT images during water drop condensation on sand grains. By doing that it would be possible to measure the drop's contact angles, evaluate void ratio and saturation degree and not

only capture images already in pendular or funicular states. Better quality CT images can also help to improve the contact angle measurement, since boundaries between materials are the regions most prone to segmentation error, but also the ones with higher importance to this research.

Acknowledgements

The authors acknowledge the funding of this research by the German Research Foundation (Deutsche Forschungsgemeinschaft, DFG) in the framework of Research Training Group GRK 2462: Processes in natural and technical Particle-Fluid-Systems (PintPFS) at Hamburg University of Technology (TUHH).

The authors would also like to thank the Betriebseinheit Elektronenmikroskopie (BeEM) of the TUHH and Mattia Gianini, PhD, from Thermo Fisher for the ESEM analysis.

References

- Cassie, A.B.D. and S. Baxter. 1944. 'Wettability of porous surfaces', *Transactions of the Faraday Society*, 40, 546. <https://doi.org/10.1039/tf9444000546>
- Jordán, A., L. M. Zavala, J. Mataix-Solera and S. H. Doerr. 2013. 'Soil water repellency: Origin, assessment and geomorphological consequences', *CATENA*, 108, 1–5. <https://doi.org/10.1016/j.catena.2013.05.005>
- Liu, D. and S. D. N. Lourenço. 2019. 'Mechanical behaviour of polymer-coated sands', *Proceedings of the XVII European Conference on Soil Mechanics and Geotechnical Engineering*, (Geotechnical Engineering, foundation of the future), 4166–4173. <https://doi.org/10.32075/17ECSMGE-2019-0860>
- Lourenço, S.D.N., S. K. Woche, J. Bachmann and Y. Saulick. 2015. 'Wettability of crushed air-dried minerals', *Géotechnique Letters*, 5(3), 173–177. <https://doi.org/10.1680/jgele.15.00075>
- Lourenço, S. D. N., Y. Saulick, S. Zheng, H. Kang, D. Liu, H. Lin and T. Yao. 2018. 'Soil wettability in ground engineering: fundamentals, methods, and applications', *Acta Geotechnica*, 13(1), 1–14. <https://doi.org/10.1007/s11440-017-0570-0>
- Milatz, M., N. Hüsener, E. Andò, G. Viggiani and J. Grabe. 2021. 'Quantitative 3D imaging of partially saturated granular materials under uniaxial compression', *Acta Geotechnica*, 16(11), 3573–3600. <https://doi.org/10.1007/s11440-021-01315-5>
- Schroeter, B., I. Jung, K. Bauer, P. Gurikov and I. Smirnova. 2021. 'Hydrophobic Modification of Biopolymer Aerogels by Cold Plasma Coating', *Polymers*, 13(17), 3000. <https://doi.org/10.3390/polym13173000>
- Zainal, M.N.F., N. Redzuan, and M. Misnal. 2015. 'Brief review: Cold plasma', *Jurnal Teknologi*, 74, 57–61. <https://doi.org/10.11113/jt.v74.4834>